Antimicrobial PLA/TPS/gelatin sheets with enzymatically crosslinked surface containing silver nanoparticles

Ana Paula De Oliveira Pizzoli,[1] Nicolli Grecco Marchiore,[2] Silvio José De Souza,[2] Priscila Dayane de Freitas Santos,[2] Odinei Hess Gonçalves,[1] Fabio Yamashita,[3] Livia Bracht,[2] Marianne Ayumi Shirai,[1] Fernanda Vitória Leimann[1]

[1]Programa De Pós-Graduação Em Tecnologia De Alimentos, Universidade Tecnológica Federal Do Paraná, Campus Campo Mourão (UTFPR-CM), via Rosalina Maria Dos Santos, 1233, CEP 87301-899, Caixa Postal: 271, Campo Mourão, Paraná, Brazil

[2]Departamento Acadêmico De Alimentos, Universidade Tecnológica Federal Do Paraná, Campus Campo Mourão (UTFPR-CM), via Rosalina Maria Dos Santos, 1233, CEP 87301-899, Caixa Postal: 271, Campo Mourão, Paraná, Brazil

[3]Departamento De Ciência E Tecnologia De Alimentos, Centro De Ciências Agrárias, Universidade Estadual De Londrina (UEL), Rod. Celso Garcia Cid (PR 445), Km 380, Caixa Postal 10.011, CEP: 86057-970, Londrina, Paraná, Brazil

Correspondence to: F. V. Leimann (E-mail: fernandaleimann@utfpr.edu.br)

ABSTRACT: In the present work, poly (lactic acid)/thermoplastic starch/gelatin sheets were produced by calendering–extrusion process and silver nanoparticles (AgNPs, synthesized by chemical reduction with D-glucose), were incorporated at sheet surfaces to promote antimicrobial activity. A gelatin solution containing AgNPs was enzymatically crosslinked as a layer at sheets surface using transglutaminase. AgNPs presented 63 nm (z average size) and spherical shape (scanning electron microscopy, SEM) while morphology analysis showed that sheets presented internal porosity. Mechanical properties (Young modulus, elongation at break, and tensile strength) and water vapor permeability presented significant difference in function of gelatin amount added to sheets formulation due to increased internal porosity. Antimicrobial activity was demonstrated against *Bacillus cereus*, *Staphylococcus aureus*, *Escherichia coli*, and *Pseudomonas aeruginosa* for the AGNPs solution as well as for the surface treated films. © 2015 Wiley Periodicals, Inc. J. Appl. Polym. Sci. **2016**, *133*, 43039.

INTRODUCTION

The main function of food packaging is to maintain products quality and safety during storage and transportation extending their shelf life. This can be achieved by preventing the contact of the food with unfavorable factors or conditions, such as microorganisms, chemical contaminants, oxygen, moisture and light. Thus, packaging materials provide physical protection and create appropriate physical and chemical conditions for food products.[1] Packaging materials used for food products, as any other type of short-term storage container, are a serious environmental problem[2] so the use of biodegradable polymers in this area represents an interesting alternative.[3] Poly (lactic acid) (PLA), thermoplastic starch (TPS), gelatin, chitosan, and poly(caprolactone) (PCL) have been extensively investigated for packaging applications.[4] Another point to be noted is that besides their biodegradability packing materials produced with biopolymers are excellent vehicle for the incorporation of a variety of additives such as antioxidants, antifungal agents, antimicrobial agents, pigments, and other nutrients.[5]

The production of packaging with antimicrobial properties is an option to inhibit microbial growth in food stuff instead of the traditional addition of antimicrobial agents to food formulations. It is well known that the latter is not always efficient, since antimicrobial protection capacity may be neutralized by reactions and/or interactions with the complex food composition. Furthermore, degradation reactions occur more intensively on food surface so the addition of the antimicrobial compound in the whole food is not required. Active packaging containing the antimicrobial agent is an alternative in this case, allowing the controlled release of antimicrobial agent at a suitable rate during storage.[6] The antimicrobial properties of silver nanoparticles (AgNPs) have been increasingly explored in consumer

Additional Supporting Information may be found in the online version of this article.

products such as deodorants, clothing, as well as cleaning solutions and sprays.[7,8] Its application in food packaging[9,10] and edible films[11] has been the subject of many studies since silver has a broad antimicrobial spectrum of activity being active against Gram-negative and Gram-positive bacteria, fungi, protozoa, and certain viruses[12] even in extremely low concentrations.

Some strategies have been employed for the incorporation of antimicrobial agents to polymer films. Most often, films can be produced by casting and the antimicrobial agent is incorporated directly into the film forming solution.[13,14] In the case of extrusion, antimicrobial agent can be incorporated directly during the material processing.[15] However, strategies to apply antimicrobial agents only at package surfaces demand investigation in order to minimize interaction with food components as well as the amount of antimicrobial agent used.

The layer-by-layer technique has emerged as a promising tool for the functionalization of a variety of substrates due to their ease of formation and flexibility to adapt physicochemical properties.[16] As an example, surface modification of polymeric materials by crosslinking chitosan hydrogels[17] and biofilm deposition containing an antibiotic[18] have also been applied to create antimicrobial materials.

In this context, the development of active biodegradable packaging with antimicrobial properties obtained by surface modification must be better investigated. In the present work PLA/TPS/gelatin sheets were produced by calendering–extrusion process and their surface was modified by the deposition of an enzymatically crosslinked gelatin hydrogel containing AgNPs.

MATERIALS AND METHODS

Materials

Soluble starch (Merk, GR grade), D-glucose (Isofar), and silver nitrate (Proquímicos) were used to AgNPs synthesis. Sheets were produced with cassava starch (Indemil), glycerol (Dinâmica), gelatin (Dinâmica), and PLA (Ingeo 4043D, Natureworks LLC). Magnesium nitrate, calcium chloride and sodium chloride (Vetec) were used to control the relative humidity during sheets conditioning. Transglutaminase (Activa WM®), kindly supplied by Ajinomoto was used to surface modification of the extruded sheets.

Microorganisms

All standard microorganisms were provided by the Adolfo Lutz Institute, Sao Paulo, Brazil. The tests included Gram-positive bacteria: *Bacillus cereus* (ATCC 14579) and *Staphylococcus aureus* (ATCC 6538); and Gram negative bacteria *Escherichia coli* (ATCC 25922) and *Pseudomonas aeruginosa* (ATCC 9027). Bacteria were grown in Mueller–Hinton broth (Biomark) at 37°C for 24 h and maintained on slopes of nutrient agar (Biomark).

Silver Nanoparticles Synthesis and Characterization

The procedure adopted to synthesize AgNPs was previously described by Ghaseminezhad *et al.*[19] Initially, 2 mL of a silver nitrate aqueous solution (25 mM) was mixed with 50 mL starch solution (1%, w/w) and 4 mL aqueous D-glucose (25 mM) was added. Finally, the resultant solution was autoclaved (121°C and

Table I. Composition of the PLA/TPS/Gelatin Extruded Sheets

Formulation	PLA (%)	Starch (%)	Glycerol (%)	Gelatin (%)
AgS1	50.0	37.1	12.4	0.5
AgS3	50.0	36.4	12.1	1.5
AgS5	50.0	35.6	11.9	2.5

15 psi) for 15 min resulting in silver colloidal nanoparticles solutions.

The nanoparticle sizes distribution and z-average size of the synthesized AgNPs were determined by dynamic light scattering (DLS, Malvern Zetasizer Nano S). Plasmon absorption analysis was performed using an UV–Vis spectrophotometer (OCEAN OPTICS, USB650UV) and the full-width at half maximum (FWHM) was determined to estimate nanoparticles size.[20] Morphological analysis of AgNPs was performed by scanning electron microscopy (SEM, Shimadzu SSX 550 Superscan). The characterization of functional groups on the surface of AgNPs was carried out by Fourier-transform infrared spectroscopy (FTIR) (IR AFFINITY-1, Shimadzu), and the spectra were scanned in the 500–4000 cm^{-1} range at a resolution of 4 cm^{-1}.The total concentration of metallic silver was determined by inductively coupled plasma mass spectrometry (ICP-MS, Perkin Elmer, D 300 Nexion). AgNPs solution obtained in the synthesis was diluted 200 times before injection.

AGNP$_S$ Antimicrobial Activity

The minimum inhibitory concentration (MIC) of the AGNPs was determined by standard microdilution technique using sterile 96-well microtiter plates.[21] Initially 100 μL of Mueller–Hinton broth was added into each well. Then, 100 μL of the AGNP solution was added to the first well and serial twofold dilutions were made down obtaining different concentration of AGNP solution (67.81; 33.90; 16.95; 8.47; 4.23; 2.11; 1.06; 0.53; 0.26; 0.13; 0.06; 0.03 mg·L^{-1}). The bacterial inoculum was prepared in Mueller–Hinton broth at a density adjusted per tube to 0.5 of the McFarland scale (10^8 bacterial cells) and diluted 1:10 for the broth microdilution procedure. Then, 5 μL of this bacterial suspension was inoculated into each well. Finally, microtiter plates were incubated at 37°C for 24 h. The MIC was defined as the lowest concentration of AGNP that inhibited visible growth compared with the control.

PLA/TPS/Gelatin Extruded Sheets Production

The procedure adopted was described by Shirai *et al.*[22] with some modifications (Table I). Gelatin percentage (wt %) is related to TPS mass (starch and glycerol). The proportion between starch and glycerol was kept constant in all formulations (33 g glycerol/100 g starch).

Initially, gelatin was allowed to gelatinize in contact with glycerol during 24 h at room temperature for sheets productions. Then, starch and PLA were added, mixed, and extruded as cylindrical profiles in a single-screw extruder (BGM, EL-25 model, Brazil) using the following processing conditions: screw diameter of 25 mm, screw length of 28 D, screw speed of

30 rpm, and temperature profile of 90/180/180/180°C at the four heating zones. The extruded cylindrical profiles were cooled at room temperature and pelletized.

Pellets were extruded in a pilot co-rotating twin-screw extruder (BGM, D-20 model) coupled with a calender (AX-Plasticos, Brazil) for sheets production. The processing conditions employed were: screws diameter (D) of 20 mm, screws length of 35 D, temperature profile of 100/170/170/170/175°C, screw speed of 100 rpm, and feed speed of 30 rpm. In the calender, the distance between the rolls was 0.8 mm and the roll speed was adjusted depending on the formulation to maintain continuous processing.

AGNPs Incorporation on the Sheets Surface

To incorporate AgNPs at sheets surface an aqueous solution containing gelatin (0.8 wt %) and transglutaminase (1 wt %) was added to silver colloidal nanoparticles dispersion, to reach the MIC of the AGNPS determined to the most resistant microorganism as described above. The resulting solution was placed in a tray and the previously cut sheets (10 cm × 20 cm) were dipped into the AgNPs solution for 30 s. Then, the treated sheets were dried at room temperature during 24 h.

Sheets Characterization

Thickness and Density. Sheets thickness was determined with the use of a digital micrometer (Starrett, 0.001 mm resolution). Ten random points were measured from each sample. To determine density, samples (20 × 20 mm) were kept in a desiccator containing anhydrous calcium chloride (0% relative humidity) for 2 weeks and then weighted.[23]

Moisture Content. Sheets were weighted (mi_1) and accondi-tioned in a circulation air oven for 24 h at 70°C. After that sheets were weighted again (ms_1) and humidity (%) was calculted using eq. (1).

$$U = \frac{(mi_1 - ms_1)}{mi_1} 100 \tag{1}$$

Water Solubility. Water solubility is defined as the dry mass content from the sheets that was solubilized after 24 h of immersion in water at 25°C. The procedure adopted was described by Soares et al.[17] Sheet samples (2 × 2 cm) were weighted (mi_2) and then immersed in water (200 mL, 25 ± 2°C) for 24 h. After that the residual sheet was removed and dried at 70°C in a forced air oven for 24 h. The samples were then weighed (ms_2) and water solubility (%) was calculated using eq. (2), where m_a is the mass of water calculated from the humidity, and ($mi_2 - m_a$) the initial mass of the sheet on dry basis.

$$SOL = \frac{((mi_2 - m_a) - ms_2)}{(mi_2 - m_a)} .100 \tag{2}$$

Water Vapor Permeability (WVP). The water vapor permeability of the sheets was determined in appropriate aluminum diffusion cells, using a relative humidity (RH) of 2% inside the cell and 75% outside the cell (ASTM E 96-00). All tests were carried out in triplicate.

Moisture Sorption Isotherm. The moisture sorption isotherms of the sheets were obtained by the static gravimetric method using saturated saline solutions (11.8, 32.8, 52.9, 75, and 87%) to promote different values of relative humidity. The sheets
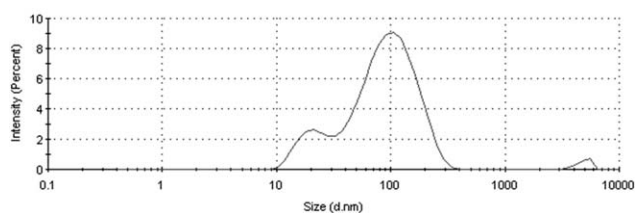

Figure 1. Particle sizes distribution by intensity of the synthesized AgNPs.

were previously dried in desiccator containing anhydrous calcium chloride (0% relative humidity) for 2 weeks, and then maintained in closed recipients with the different saturated saline solution at 25°C. The samples were weighed in regular intervals until three equal weight measurements were obtained (equilibrium condition). The absolute humidity (dry base) was determined by the oven method (105°C for 24 h) in triplicate. GAB (Guggenheim–Anderson–de Boer) model [3] was used to fit the experimental data. In this equation, parameter X_w is the equilibrium moisture content (g water/g dry solid) at a known water activity (a_w), m_0 is the monolayer water content, C is the Guggenheim constant (representing the sorption heat of the first layer), and k is the sorption heat of the multilayer. The parameters of the GAB model were determined using nonlinear regression performed using Statistica 7.0 (Stat-Soft).

$$X_w = \frac{m_0.C.K.a_w}{(1 - K.a_w).(1 - K.a_w + C.K.a_w)} \tag{3}$$

Mechanical Properties. The tensile strength tests were performed with a texture analyzer (Stable Micro Systems, TA XT plus model) based on the American Society for Testing and Material Standards (ASTM, 2002). Ten samples (10 × 100 mm) of each formulation were previously conditioned at 23 ± 2°C and 53 ± 2% of relative humidity for 48 h. The properties measured were tensile strength (MPa), elongation at break (%), and Young's modulus (MPa). Ten samples were tested for each formulation.

Scanning Electron Microscopy (SEM). The microstructure of the surface and fractured sheets was analyzed with a scanning electron microscope (Philips, XL-30 model) with electron source of tungsten and detectors of secondary and backscattered electrons at 20 kV. Sheets were immersed in liquid nitrogen and then fractured. The samples were gold coated using a sputter coater (BALTEC, SCD 005 model).

Sheets Antimicrobial Activity. Antimicrobial activity was evaluated using the agar disk diffusion method. Circular samples of the sheets (2 mm diameter) were placed in Petri dishes containing Mueller–Hinton agar. The bacterial cultures concentration in the inoculum was 10^8 CFU·mL^{-1} (McFarland scale 0.5).[8] The Petri dishes were then incubated at 37°C for 24 h. The antimicrobial activity of the sheets was evaluated by measuring the diameter (mm) of the growth inhibition zone. The experiment was carried out in duplicate for each formulation.

Statistical Analysis. The obtained results were evaluated using analysis of variance (ANOVA), and treatment averages were compared using Tukey's test at the 5% significance level ($P < 0.05$) using the software Statistica 7.0.
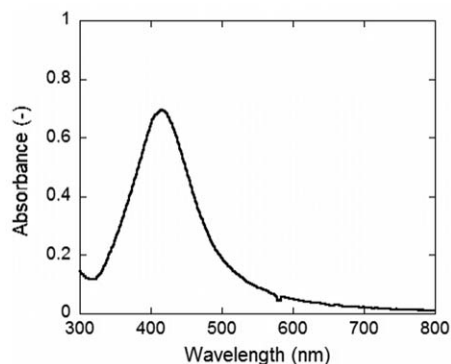
Figure 2. UV–Vis spectrum of the AgNPs colloidal suspension.

RESULTS AND DISCUSSION

AGNPs Characterization

Particle sizes distribution by intensity is presented in Figure 1. UV–Vis spectrum of the nanoparticles colloidal suspension, their morphology by SEM image and FTIR spectra are presented in Figures 2, 3, and 4, respectively.

The colloidal suspension of AgNPs was analyzed by ICP-MS and the result indicated that the real concentration of silver nanoparticles present in the solution was equal to 135.62 ± 1.28 mg L^{-1}. Z-average diameter (Dz) determined by DLS of the AgNPs was equal to 63 nm, which is in fair agreement with the SEM image (Figure 4). It is possible to observe the surface plasmon resonance (SPR) peak at 410 nm (Figure 2 and Supporting Information Table SI). According to Bankura et al.[24] silver nanoparticles absorb radiation at visible range (380–450 nm) and a well defined peak is an indicative of an adequate degree of dispersion as well as nanoparticles with spherical shape and narrow sizes distribution[25,26] which can be observed in the SEM images. Polydispersity index obtained by DLS was equal to 0.44 indicating a large size distribution which could be attributed to nanoparticles agglomeration as observed in the microscopy image. AgNPs agglomerates are about 300–400 nm (according to the SEM image) corresponding to the great peak found by DLS (Figure 1). The second peak (3,000 to
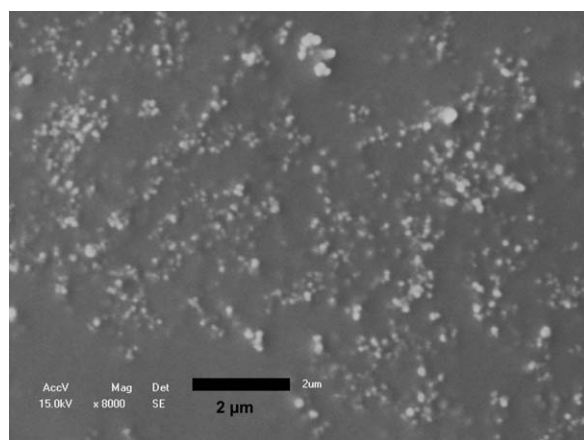

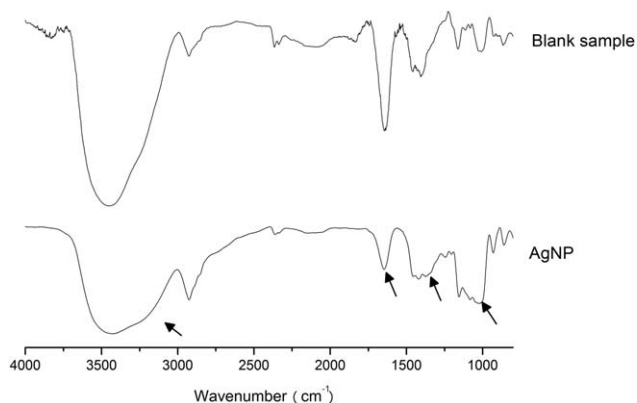**Figure 3.** Scanning electron microscopy image of the synthesized AgNPs (8,000×).

Figure 4. FTIR spectra of: blank sample (starch and glucose), and silver nanoparticles (AgNP synthesized with glucose and starch).

6,000 nm) is small and can be related to impurities, such as dust.[27]

Full-width at half maximum method (FWHM) resulted in an average particle diameter equal to 100 nm. Zielinska et al.[28] obtained silver nanoparticles using chemical reduction techniques presenting FWHM values from 5 to 100 nm. An et al.[11] used the borohydride technique and obtained 20 nm AgNPs. Ghaseminezhad et al.[19] also obtained a FWHM value of 20 nm using the same technique applied at the present work.

At the FTIR spectra presented at Figure 4 one can observe that the blank sample (without the addition of silver nitrate) and synthesized AgNPs present different intensities on the characteristic bands of the O—H stretching (3400 cm^{-1}), C═O (1600 cm^{-1}), C—O—H (1350 cm^{-1}), and CO (1000 cm^{-1}) in function of their interaction with AgNPs.[29,30] The O—H groups of starch have the ability of coordination reaction with metal ions (e.g., with silver ions) and in the presence of silver ions form coordination bonds.[29]

Table II presents the minimum inhibitory concentration (MIC) results of the aqueous AgNPs dispersion. AGNPs were effective in inhibiting both Gram positive (*Bacillus cereus* and *Staphylococcus aureus*) and Gram negative (*Escherichia coli* and *Pseudomonas aeruginosa*) microorganisms. *Staphylococcus aureus* presented the higher resistance to AgNPs action (MIC equal to 37.50 μg mL^{-1}) while the lower resistance to AgNPs inhibitory effect was observed for *E. coli*. Similar results were observed by Martínez-Castañón et al.[31] The difference between the inhibitory concentration between Gram positive and Gram negative microorganisms can be attributed to the microorganisms cellular wall structure.[32] Gram negative microorganisms cellular wall

Table II. Minimum Inhibitory Concentration (MIC) of the Colloidal AgNPs Solution

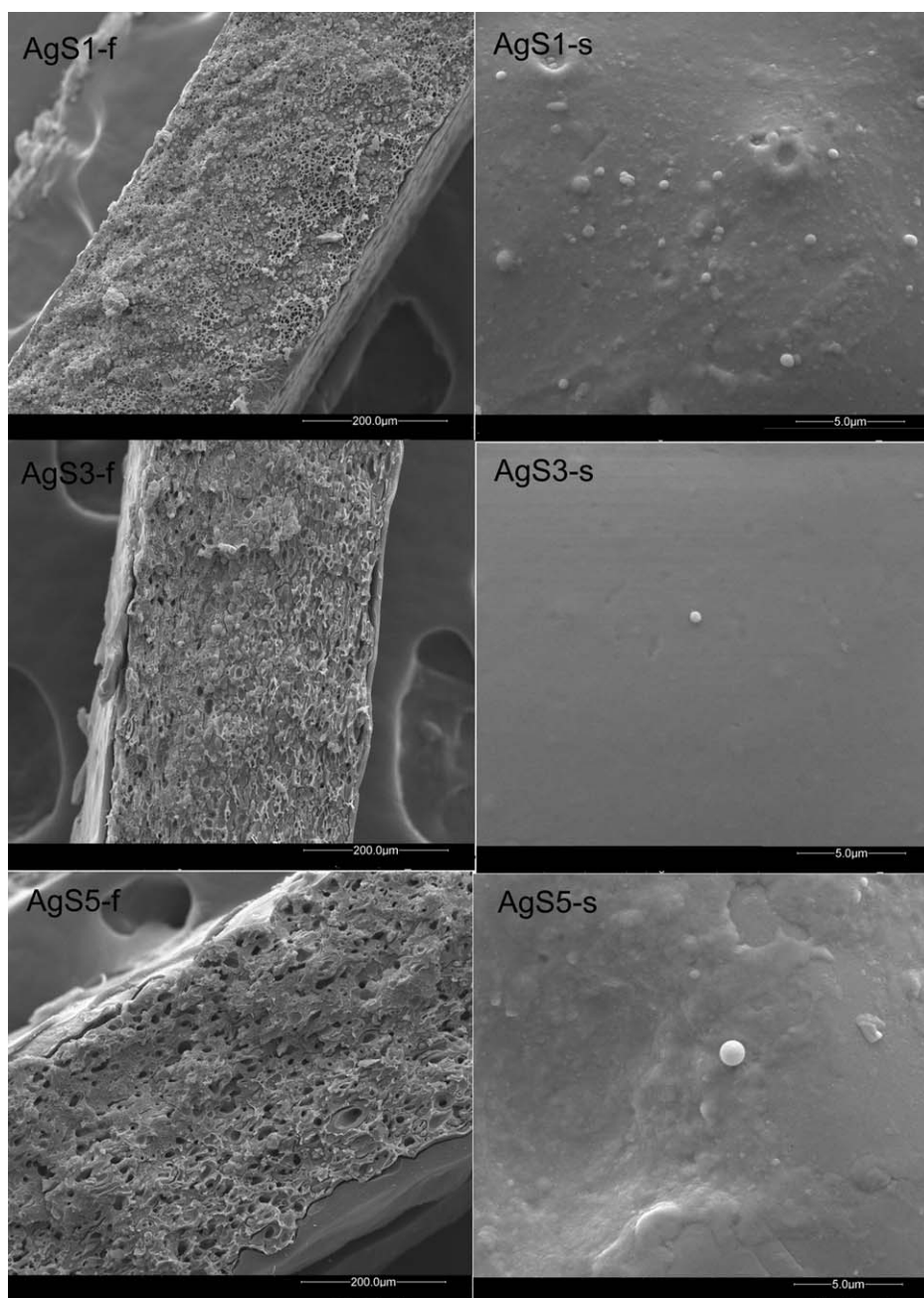| Microorganism	MIC (μg mL^{-1})
Bacillus cereus (ATCC 14579)	2.34
Staphylococcus aureus (ATCC 6538)	37.50
Escherichia coli (ATCC 25922)	1.17
Pseudomonas aeruginosa (ATCC 9027)	4.69

Figure 5. Scanning electron microscopy images of the surface treated PLA/TPS/gelatin sheets containing AgNPs: AgS1, formulation with 1% of gelatin; AgS3, formulation with 3% of gelatin and AgS5, formulation with 5% of gelatin (*f* fracture 400× magnification and *s* surface 12,000× magnification).

is composed by a thin peptidoglycan layer and a lipopolysaccharide layer that act as a weak permeability barrier to AgNPs. In contrast, Gram positive microorganism cellular wall is composed by a thick peptidoglycan layer consisting of linear polysaccharide chains crosslinked by short peptides. This is a rigid three-dimensional structure making AgNPs penetration and absorption more difficult.

Sheets Characterization

At Figure 5, SEM images of the AgNPs surface treated sheets are presented. It is possible to note the presence of starch granules and an increase in the porosity in the fractures for increasing gelatin amount. This can be attributed to the fact that during the treatment with AgNPs and the crosslinking step there was a rearrangement of the polymeric matrix in the sheets due to the presence of water and the increase of gelatin amount promoting a more porous structure. In the fracture images, it is also possible to observe a thin layer on sheets surface created by the crosslinked gelatin containing the AgNPs. The difference between the thicknesses of these structures is due to the position that the sheets kept during the crosslinking and drying step. It is possible to note that these structures are peeling from

Table III. Thickness, Density, WVP, Moisture Content ($U\%$), and Solubility (SOL %) Results Obtained for the Surface Treated PLA/TPS/Gelatin Sheets Containing AgNPs

Formulation	Thickness (μm)	Density (g/cm^3)	U (%)	WVP (g m^{-1} Pa^{-1} dia^{-1}) ($\times 10^{-6}$)	SOL (%)
AgS1	487 ± 6	1.29 ± 0.13	4.39 ± 1.78	4.86[a] ± 4.50	11.44[a] ± 0.65
AgS3	410 ± 2	1.36 ± 0.01	5.73 ± 0.28	5.14[a] ± 1.28	20.34[b] ± 2.09
AgS5	396 ± 15	1.12 ± 0.05	5.44 ± 0.18	6.93[b] ± 1.68	27.72[b] ± 2.79

a, b, c, d means followed by the same letters in the column did not show differences at 5% of significance level according to Tukey's test.

Table IV. Mechanical Properties of Surface Treated PLA/TPS/Gelatin Sheets Containing AgNPs

Formulation	Tensile strength (MPa)	Elongation at break (%)	Young's modulus (MPa)
AgS1	21.6[a] ± 5,2	7.5[a] ± 3,8	477 ± 88
AgS3	19.0[a,b] ± 3,3	7.1[a] ± 1,7	471 ± 45
AgS5	15.9[b] ± 5,1	3.6[b] ± 1,7	437 ± 89

a, b, c, d means followed by the same letters in the column did not show differences at 5% of significance level according to Tukey's test.

the sheets matrix. Ichinose et al.[33] also observed peeling structures at ultrathin crosslinked films produced by layer-by-layer technique with poly(allylamine hydrochloride), poly(vinyl methyl ether), and monomethyl maleate crosslinked with glutaraldehyde.

Values for thickness, density, WVP, moisture content, and solubility are presented at Table III. Mechanical properties results determined for the surface treated sheets are presented at Table IV. Thickness, density, and moisture content results did not differed significantly showing that the experimental condition was uniform for all samples. The 5% increase in the gelatin amount in sheets formulation promoted an increase in water vapor permeability ($P < 0.05$). Similar results were also obtained for gelatin/casein films crosslinked with transglutaminase.[34] The effect was attributed to the organization degree of protein polymer network, since molecules with bulky chains, like proteins, have

a lower packaging degree, thus enabling a greater permeability. Gelatin crosslinking on the sheet surface created an open structure possibly affecting water vapor permeability. Furthermore, this result is in agreement with the SEM analysis, taking into account that the internal microstructure of the sheets produced with 5% of gelatin presented higher porosity.

Water solubility of the sheets increased with the increase in gelatin amount in the formulation ($P < 0.05$). This may be related to the previous gelatinization of gelatin with glycerol before the extrusion process. Gelatin chains were completely dispersed in the sheets structure while starch presented granular structures at SEM micrographs (Figure 5). Solubilization of gelatin as well as glycerol from the treated sheets occurs easier than for starch granules since gelatin was in an amorphous state in the sheets structure.

Young's Modulus was not significantly affected ($P > 0.05$) by the amount of gelatin used. Shirai et al.[35] have found values in the range of 10 MPa for PLA/TPS extruded sheets obtained using the same equipment and experimental conditions used at the present work. The presence of crosslinked gelatin on the sheets surface promoted a substantial increase in the Young's modulus enhancing materials strength.[36] Elongation at break decreased
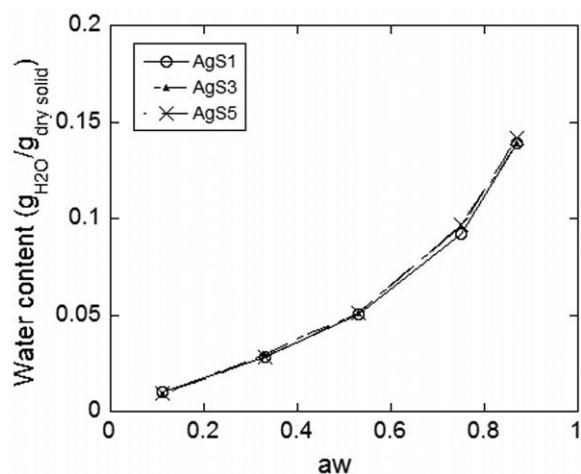
Figure 6. Moisture sorption isotherm for the surface treated PLA/gelatin sheets containing AgNPs.

Table V. GAB Model Parameters for Moisture Sorption Isotherms of Surface Treated PLA/TPS/Gelatin Sheets Containing AgNPs

Parameter	AgS1	AgS3	AgS5
C	2.78	2.05	2.01
K	0.86	0.81	0.82
m_0	0.039	0.049	0.048
R^2	0.99	0.99	0.99

m_0 = monolayer water content; C = Guggenheim constant; K = sorption heat of the multilayer; R^2 = correlation coefficient.

Table VI. Antimicrobial Activity of Surface Treated PLA/TPS/Gelatin Sheets Containing AgNPs (5% Gelatin, AgS5)

Microorganism	Inhibition zone (cm)
Bacillus cereus (ATCC 14579)	0.50 ± 0.00
Staphylococcus aureus (ATCC 6538)	0.80 ± 0.10
Escherichia coli (ATCC 25922)	0.40 ± 0.00
Pseudoman asaeruginosa (ATCC 9027)	0.60 ± 0.10

when 5% gelatin was used (AgS5). This behavior could be related to the increase of crosslinking points between gelatin and sheets surface leading to a greater number of stress concentration points. Cao et al.[37] produced gelatin films crosslinked with ferulic and tannic acid and also observed a reduction in elongation at break. Tensile strength also decreased for increasing amounts of gelatin ($P < 0.05$). The reduction in tensile strength of AgS5 formulation can be related to internal porosity as detected by SEM (Figure 5).

The sorption isotherm and Guggenheim, Anderson, and De Boer (GAB) model are presented in Figure 6 and Table V, respectively. The three samples presented a J-shape behavior at the sorption isotherm. According to Lim et al.[38] this result suggests the formation of water clusters into the polymeric matrix as water activity increases. The strong function of equilibrium moisture content with water activity could be attributed to swelling of the biopolymer matrix, which may have caused an exposure of more water binding sites for water sorption. The highest water content obtained for all samples was equal to 0.16 $g_{H2O}/g_{dry\ solid}$. Carvalho et al.[39] have found a maximum water content of 0.55$g_{H2O}/g_{dry\ solid}$ while[38] found 0.40 $g_{H2O}/g_{dry\ solid}$ for gelatin enzymatically crosslinked films. The lower value found at this work could be attributed to the hydrophobic character of PLA present in the sheets matrix.

The experimental data presented a satisfactory adjustment to the GAB model ($R^2 > 0.99$). The m_0 values found for the formulations with higher gelatin amount (AgS3 and AgS5) were greater indicating that the films adsorbed more water at the monolayer. K decreases with increasing gelatin concentration in sheets because the material became more hydrophilic so a higher number of interactions between water vapor and the film could take place creating adsorbed multilayers. C parameter is associated with the sorption heat of the monolayer. C values are consistent with values found in other studies where starch and gelatin based materials.[22,40]

Antimicrobial activity of the surface treated sheets against *Bacillus cereus*, *Staphylococcus aureus*, *Escherichia coli*, and *Pseudomonas aeruginosa* are shown in Table VI. The inhibition halo was formed for all bacteria analyzed demonstrating that AgNPs continued to act as antimicrobial agent even after being incorporated at sheets surface by crosslinked gelatin. Galya et al.[41] silver nitrate and the inhibition halos obtained ranged from 0.5 to 0.9 cm against *E. coli* depending on the concentration of antimicrobial agent incorporated in the film. Hsu et al.[42] produced chitosan films containing AgNPs and observed an inhibition halo equal to 0.6 cm against *Staphylococcus aureus*.

CONCLUSIONS

Silver nanoparticles were successfully synthesized using an environmental friendly process and presented effective antimicrobial action against Gram positive and Gram negative microorganisms. PLA/TPS/gelatin sheets were obtained and surface treated with a solution containing gelatin, transglutaminase, and the AgNPs, forming a crosslinked antimicrobial surface. The formulation containing 5% gelatin showed higher porosity leading to higher water vapor permeability, lower tensile strength, and elongation at break, and increased hydrophilicity. The antimicrobial activity of the surface treated sheets containing AgNPs was confirmed by the formation of inhibition zones against *Bacillus cereus*, *Staphylococcus aureus*, *Escherichia coli*, and *Pseudomonas aeruginosa*. The obtained PLA/TPS/gelatin sheets have a great potential to be used as active packaging for food conservation.

REFERENCES

1. Rhim, J. W.; Park, H. M.; Ha, C. S. *Prog. Polym. Sci.* **2013**, *38*, 1629.

2. Kirwan, M. J.; Strawbridge, J. W. *Food Packag. Technol.* **2003**.

3. Bordes, P.; Pollet, E.; Averous, L. *Prog. Polym. Sci.* **2009**, *34*, 125.

4. Yu, L.; Dean, K.; Li, L. *Prog. Polym. Sci.* **2006**, *31*, 576.

5. Imran, M.; El-Fahmy, S.; Revol-Junelles, A. M.; Desobry, S. *Carbohydr. Polym.* **2010**, *81*, 219.

6. Appendini, P.; Hotchkiss, J. H. *Innov. Food Sci. Emerg. Technol.* **2002**, *3*, 113.

7. Rai, M.; Yadav, A.; Gade, A. *Biotechnol. Adv.* **2009**, *27*, 76.

8. Suppakul, P.; Sonneveld, K.; Bigger, S. W.; Miltz, J. *J. Food Eng.* **2011**, *105*, 270.

9. Fortunati, E.; Armentano, I.; Zhou, Q.; Iannoni, A.; Saino, E.; Visai, L.; Berglund, L. A. *Carbohydr. Polym.* **2012**, *87*, 1596.

10. Lloret, E.; Picouet, P.; Fernández, A. *LWT Food Sci. Technol.* **2012**, *49*, 333.

11. An, J.; Zhang, M.; Wang, S.; Tang, J. *LWT Food Sci. Technol.* **2008**, *41*, 1100.

12. Kumar, R.; Münstedt, H. *Biomaterials* **2005**, *26*, 2081.

13. Ehivet, F. E.; Min, B.; Park, M.; Oh, J. *J. Food Sci.* **2011**, *76*.

14. Lara-Lledó, M.; Olaimat, A.; Holley, R. A. *Int. J. Food Microbiol.* **2012**, *156*, 25.

15. Pires, M.; Petzhold, C. L.; Santos, R. V.; Perão, L.; Chies, A. P. *Polímeros* **2014**, *24*, 237.

16. Yamanlar, S.; Sant, S.; Boudou, T.; Picart, C.; Khademhosseini, A. *Biomaterials* **2011**, *32*, 5590.

17. Soares, F. C.; Yamashita, F.; Müller, C. M. O.; Pires, A. T. N. *Polym. Test.* **2013**, *32*, 94.

18. Kowalczuk, D.; Ginalska, G.; Golus, J. *Int. J. Pharm.* **2010**, *402*, 175.

19. Ghaseminezhad, M. S.; Hamedi, S. A.; S. *Carbohydr. Polym.* **2012**, *89*, 467.

20. Munger, M.; Radwanski, P.; Hadlock, G. C.; Stoddard, G.; Shaaban, A.; Falconer, J.; Grainger, D. W.; Deering-Rice, C. E. *Nanomedicine* **2014**, *10*, 1.

21. CLSI. *Clin. Lab. Stand. Inst.* **2005**.

22. Shirai, M. A.; Müller, C. M. O.; Grossmann, M. V. E.; Yamashita, F. *J Polym. Environ.* **2014**. doi:10.1007/s10924-014-0680-9.

23. Müller, C. M. O.; Laurindo, J. B.; Yamashita, F. *Carbohydr. Polym.* **2012**, *89*, 504.

24. Bankura, K. P.; Maity, D.; Mollick, M. M. R.; Mondal, D.; Bhowmick, B.; Bain, M. K.; Chakraborty, A.; Sarkar, J.; Acharya, K.; Chattopadhyay, D. *Carbohydr. Polym.* **2012**, *89*, 1159.

25. Song, J. Y.; Kim, B. S. *Bioprocess Biosyst. Eng.* **2009**, *32*, 79.

26. Wilcoxon, J. P.; Abrams, B. L. B. L. *Chem. Soc. Rev.* **2006**, *35*, 1162.

27. Panáček, A.; Kvítek, L.; Prucek, R.; Kolář, M.; Večeřová, R.; Pizúrová, N.; Sharma, V. K.; Nevěčná, T.; Zbořil, R. *J. Phys. Chem. B* **2006**, *110*, 16248.

28. Zielinska, A.; Skwarek, E.; Zaleska, A.; Gazda, M.; Hupka, J. *Procedia Chem.* **2009**, *1*, 1560.

29. Pandey, S.; Goswami, G. K.; Nanda, K. K. *Int. J. Biol. Macromol.* **2012**, *51*, 583.

30. Sreeram, K. J.; Nidhin, M.; Nair, B. U. *Bull. Mater. Sci.* **2008**, *31*, 937.

31. Martínez-Castañón, G. A.; Niño-Martínez, N.; Martínez-Gutierrez, F.; Martínez-Mendoza, J. R.; Ruiz, F. *J. Nanoparticle Res.* **2008**, *10*, 1343.

32. Sondi, I.; Salopek-Sondi, B. *J. Colloid Interface Sci.* **2004**, *275*, 177.

33. Ichinose, I.; Mizuki, S.; Ohno, S.; Shiraishi, H.; Kunitake, T. *Polym. J.* **1999**, *31*, 1065.

34. Chambi, H.; Grosso, C. *Food Res. Int.* **2006**, *39*, 458.

35. Shirai, M. A.; Grossmann, M. V. E.; Yamashita, F.; Garcia, P. S.; Müller, C. M. O. *Carbohydr. Polym.* **2013**, *92*, 19.

36. Anseth, K. S.; Bowman, C. N.; Brannon-Peppas, L. *Biomaterials* **1996**, *17*, 1647.

37. Cao, N.; Fu, Y.; He, J. *Food Hydrocoll.* **2007**, *21*, 575.

38. Lim, L. T.; Mine, Y.; Tung, M. A. *J. Food Sci.* **1999**, *64*, 616.

39. Carvalho, R. A.; Grosso, C. R. F. *Food Hydrocoll.* **2004**, *18*, 717.

40. Nafchi, A. M.; Alias, A. K.; Mahmud, S.; Robal, M. *J. Food Eng.* **2012**, *113*, 511.

41. Galya, T.; Sedlařík, V.; Kuřitka, I.; Novotný, R.; Sedlaříková, J.; Sáha, P. *J. Appl. Polym. Sci.* **2008**, *110*, 3178.

42. Hsu, S. H.; Chang, Y. B.; Tsai, C. L.; Fu, K. Y.; Wang, S. H.; Tseng, H. J. *Colloids Surf. B: Biointerfaces* **2011**, *85*, 198.